

## On the construction and use of a Paleo-DEM to reproduce tsunami inundation in a historical urban environment – the case of the 1755 Lisbon tsunami in Cascais

Martin Wronna, Maria Ana Baptista & Joachim Götz

To cite this article: Martin Wronna, Maria Ana Baptista & Joachim Götz (2017) On the construction and use of a Paleo-DEM to reproduce tsunami inundation in a historical urban environment – the case of the 1755 Lisbon tsunami in Cascais, *Geomatics, Natural Hazards and Risk*, 8:2, 841-862, DOI: [10.1080/19475705.2016.1271832](https://doi.org/10.1080/19475705.2016.1271832)

To link to this article: <https://doi.org/10.1080/19475705.2016.1271832>



© 2017 The Author(s). Published by Informa UK Limited, trading as Taylor & Francis Group



Published online: 18 Jan 2017.



Submit your article to this journal [↗](#)



Article views: 385



View related articles [↗](#)



View Crossmark data [↗](#)

# On the construction and use of a Paleo-DEM to reproduce tsunami inundation in a historical urban environment – the case of the 1755 Lisbon tsunami in Cascais

Martin Wronna <sup>a</sup>, Maria Ana Baptista <sup>a,b,c</sup> and Joachim Götz <sup>d</sup>

<sup>a</sup>Instituto Português do Mar e da Atmosfera, IPMA, Lisbon, Portugal; <sup>b</sup>Instituto Superior de Engenharia de Lisboa, Instituto Politécnico de Lisboa, Lisboa, Portugal; <sup>c</sup>Instituto Dom Luiz, Faculdade de Ciências da Universidade de Lisboa, Lisboa, Portugal; <sup>d</sup>Faculty of Natural Sciences, Department of Geography and Geology, University of Salzburg, Salzburg, Austria

## ABSTRACT

In this study, we present a methodology to reconstruct a Paleo Digital Elevation Model (PDEM) to simulate the propagation of a tsunami similar to the one that occurred on the 1st November 1755 in Cascais, Portugal. The method combines historical data, GPS-measurements, and present-day topographic data to build the PDEM. Antique maps were georeferenced and altitudinal information was reconstructed using historic descriptions. We used old documents to estimate the original landscape of several sites. Analyses and interpretation of these sources of information served to attribute and approximate elevations of both geomorphologic landforms and building features. We used antique maps to rebuild the boundaries of old river mouths and water courses. Finally, we use GPS-RTK to implement obtained elevation data along creek mouths to interpolate in channelled areas to get their slope. Using this methodology and a numerical tsunami simulation code, we reproduced a 1st November 1755-like flooding in Cascais, Portugal. Our results show that using the PDEM, we can reproduce the inundation described in all of the historical accounts.

## ARTICLE HISTORY

Received 28 July 2016  
Accepted 9 December 2016

## KEYWORDS

Paleo-DEM reconstruction; historical accounts; tsunami hazard assessment; antique maps

## 1. Introduction

Tsunamis have devastated coastal areas in different historical ages and represent a severe hazard potential. To better understand the tsunami hazard potential of certain areas, it is important to combine modern and historical records. Numerical simulation of tsunamis improves the hazard, the vulnerability, and the risk assessments. To do these simulations, we need accurate digital elevation models (DEMs) that include topographic and bathymetric data.

On-land propagation and the coastal inundation of historic tsunami events are difficult to simulate because of morphological and architectural changes between historic and present-day condition. Using inaccurate coastal morphology in tsunami simulation of historic events may give unreliable results. In this case, new topography and bathymetry data can serve as a basis but need to be adapted using various testimonials (e.g. historical maps and descriptions). These documents are often a valuable source of information about past landscapes and terrain morphology. However, difficulties in the interpretation of this information limit the use in quantifiable scientific studies. Blakemore and Harley (1980) defined the topographic, chronometric, and geometric accuracy as most important

aspects concerning the analysis of ancient maps. Boutoura and Livieratos (2006) summarize the most important transformation methods for comparative studies of early maps. Nowadays, digital tools allow easy access to ancient documents and facilitate their analysis and interpretation. For example, Jenny et al. (2007) present methodologies that allow to transform and rectify antique maps and to carry out accuracy analysis. James et al. (2012) present a review of methods of geomorphic change detection (GCD) using historical maps, remote sensing or ground-based topographic data and highlight the possibility to quantify geomorphological change for decadal and centennial scales. These authors also state that quality assessment of the data should be carried out for each data source as errors might propagate during DEM reconstruction. However, the examples shown in their study reach back approximately 100 years. Kormann and Lock (2013) use dynamic models to reconstruct ancient landscapes for the Helike Delta for several paleo periods. They compute the PDEMs on a relatively coarse scale taking the rate of sea level rise, the rate of vertical tectonic uplift, pulses of tectonic uplift, and subsidence, and the rate of sediment deposition into account. Information from historical accounts is implemented in one PDEM as well.

Omira et al. (2012) already used numerical tsunami modelling to test the reliability of historical accounts regarding the 1755 Lisbon tsunami in Morocco. The authors reconstructed a PDEM of the area of the old city of El-Jadida using historical maps and paying particular attention to places where significant morphological and architectural changes took place. However, they do not specify in detail how they reconstruct the PDEM on the base of these documents.

Since tsunami onshore propagation and impact in urban environments depends strongly on coastal structures, the implementation of fortifications and existing buildings in the PDEM is an important issue. Deterministic tsunami hazard assessment applies specific scenarios to study their impact on a given test site. Several studies used this scenario-based approach (e.g. Heidarzadeh et al. 2009; Omira et al. 2010; Baptista et al. 2011; Wijetunge 2014; Wronna et al. 2015) and applied the method successfully to different case studies to examine the tsunami hazard using present-day DEMs.

In this paper, we present an improved methodology for PDEM reconstruction illustrated by the case study for the coastal city of Cascais, Portugal (Figure 1). Starting with the present-day topography and bathymetry, we implement various historical data and historical maps of the study area using a geographical information system (GIS) software. Finally, we use the reconstructed PDEM in a numerical tsunami simulation for the 1st November 1755 Lisbon Earthquake and tsunami.

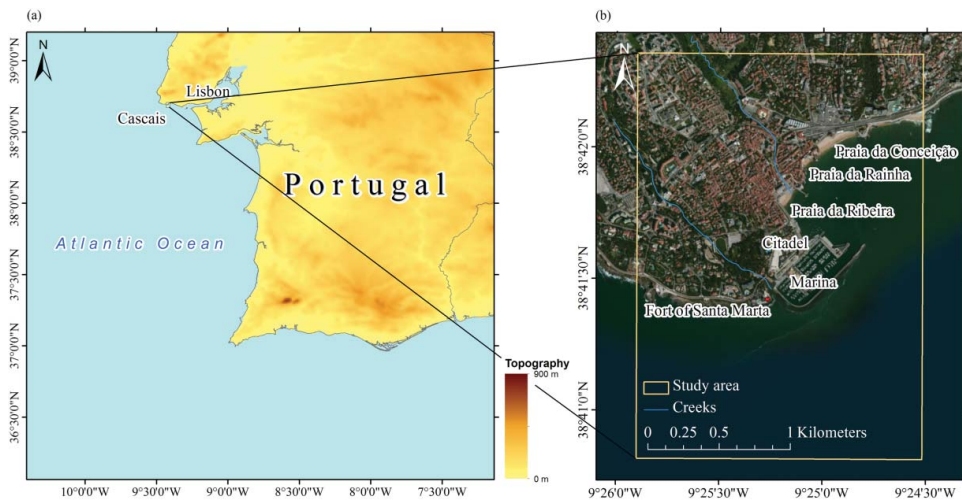


**Figure 1.** (a) Location of the study area Cascais. (b) Present-day orthophoto of Cascais city and extent of the study area and major features along the Cascais coastline.

## 2. Study area

In the morning of 1st November 1755, a massive earthquake occurred in the Atlantic southwest of Portugal and triggered a transatlantic tsunami (Martins & Mendes Victor 1990; Baptista et al. 1998a; Baptista & Miranda 2009a). The waves hit the coast of Portugal less than half an hour after the main shock causing massive inundations. As Portugal was a major colonial power at that time, the 1755 Lisbon event is probably the best-described tsunami event in the history of the 18th century.

We selected Cascais, a coastal city, located 25 km west of the Portuguese capital Lisbon (Figure 1). The study area is about 2 km wide in E–W direction and 2.8 km long in the N–S direction and lies between 9°24'40" and 9°25'55" West and 38°40'50" and 38°42'25" North. Today, the coastline forms a small bay with beaches and cliffs. The modern marina is located in front of the citadel and the fortress. There are three beaches nearby the city centre: the beaches *Praia da Ribeira*, *Praia da Rainha* and *Praia da Conceição* (Figure 1(b)). Today's city centre is located in front of the beaches *Praia da Ribeira* and *Praia da Rainha*. Presently, the vast majority of the coastal area is highly populated.

The coastal stretch west of the citadel (Figure 1(b)) presents a medium slope of approximately 10%. A slightly folded limestone forms a rocky shoreline with small cliffs and narrow incisions. The height of the cliffs increases from 6 m at the area of the citadel to 8 m at the fort of *Santa Marta* (Figure 1(b)). In between, there is a narrow sandy inlet which forms the mouth of the creek *Ribeira de Mocho*. Vegetation occurs 7–8 m above mean sea level (MSL).

## 3. Methodology of PDEM reconstruction

In the case of the 1755 event, we found historical information on the landscape of Cascais at the time of the event (Figure 1(b)). We used the historical maps to classify the areas that needed topographic reconstruction. For these areas, we used interpolation to reconstruct the topography and the morphology in the intertidal areas. Additionally, we used an antique nautical chart (Da Silva et al. 1879) as input for bathymetric reconstruction and pictures, paintings and books to estimate building heights. The amount and quality of the historical documentation of this event make it a good candidate to apply our methodology. We focused the reconstruction of the PDEM on the shallow bathymetry up to 5 m depth and topography up to 20 m height to areas prone to tsunami impact. First, we reconstructed important topographic features and, second, we introduced antique constructions.

### 3.1. Data

As primary sources of information, we used recent topographic and bathymetric data, historical maps, historical bathymetric data and historical accounts. In Table 1, we present a complete list of all the elements used for reconstruction and their contribution to the PDEM.

*Present-day topographic and bathymetric data.* The reconstruction process starts from a known or a given reference, commonly the most recent morphology of a given test site. We used a dataset containing highly accurate topographic information made available by Cascais Municipality (personal communication). This dataset contains altimetric point information and topographic contours with a spacing of 1 m. The dataset includes a point cloud, topographic and building shapes. The topographic contours have a vertical resolution of 1 m. The reference of the dataset is Datum 73 Hayford Gauss IPCC, GCS-D73, and the vertical reference system is MSL in Cascais. The actual bathymetric data is available with a resolution of 100 m and is referenced to geographic coordinates in PT-TM06/ETRS89 – European Terrestrial Reference System 1989 System – and to hydrographic zero (Instituto Hidrográfico de Portugal 2012).

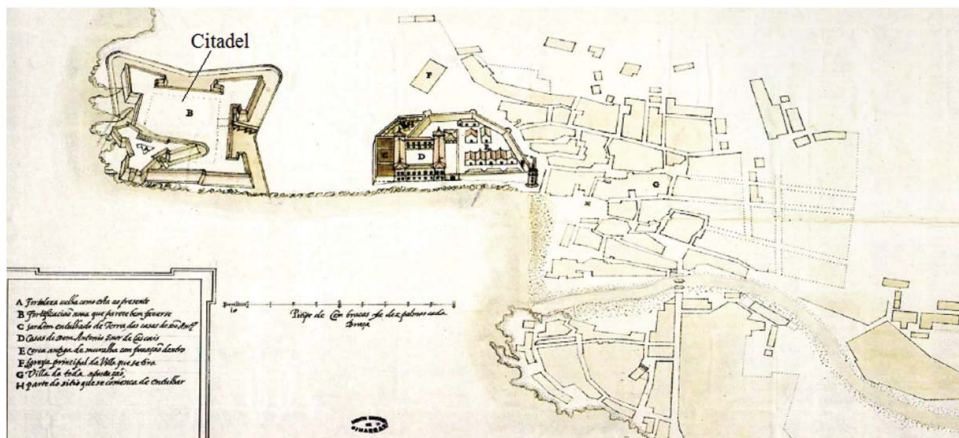
*Historical maps and hydrographic charts.* Figures 2 and 3 depict the historical maps used in chronological order. Figure 2 shows the map by Terzi (1594). It presents some important buildings: the fortress, one palace and the main church of the village behind the palace. Additionally, it depicts the

**Table 1.** Collection of data with historical information used to reconstruct the PDEM for Cascais in 1755.

Title	Source	Type	Contribution to the PDEM
Plano de Cascaes en donde figuran en perspectiva las fortalezas nueva y vieja así como las Casas de D. Antonio, señor de Cascaes	Terzi (1594)	Map	No
Plan des Vile, Citadelle et Forts de Cascaes	Weyröther (n.d., early nineteenth century)	Map	<ul style="list-style-type: none"> <li>● Coastline</li> <li>● Outline of the river mouth in the urban areas</li> <li>● Location of the constructions</li> <li>● Slope and dimensions of the beaches</li> </ul>
Plano Hydrographico da Barra do Porto de Lisboa	Da Silva et al. (1879)	Map, hydrographic chart	<ul style="list-style-type: none"> <li>● Bathymetry</li> <li>● Slope of the beaches</li> </ul>
A vile de Cascais e o terremoto de 1755	Andrade (1956)	Book	<ul style="list-style-type: none"> <li>● Constructions resisting the earthquake</li> <li>● Construction heights</li> </ul>
As Fortificações Marítimas da Costa de Cascais	Boiça et al. (2001)	Book	<ul style="list-style-type: none"> <li>● Construction heights</li> <li>● Dimensions of defensive walls</li> </ul>
Citadela de Cascais (Pedras, Homens e Armas)	Carita (2003)	Book	<ul style="list-style-type: none"> <li>● Construction heights</li> <li>● Dimensions of defensive structures</li> </ul>
Cascais em 1755. Do Terramoto á Reconstrução	Henriques (2005)	Book	<ul style="list-style-type: none"> <li>● Constructions resisting the earthquake</li> <li>● Construction heights</li> </ul>
Cascais 650 anos de História	Henriques (2014)	Book	<ul style="list-style-type: none"> <li>● Construction heights</li> <li>● Photographs used for verification of the PDEM</li> </ul>

sketch for the later built citadel commanded by King Filipe II of Spain. This map also shows one main beach and the pillars of a bridge crossing the creek *Ribeira das Vinhas* (Figure 2). However, the map illustrates the landscape of the village more than 150 years before the catastrophe. The map of Weyröther (n.d.) from the first half of the 19th century in Figure 3 includes the citadel, the forts of Cascais, and depicts the walls and fortifications along the coast.

Along with the descriptions given in historical documents, we concluded that the newer map (Figure 3) represents better the outline of Cascais in 1755, and hence we decided to use it as reconstruction reference. The map shows the contours of the fortress and the citadel and the location of important buildings at the time. Besides the size of the village, precise shapes of all the buildings are observable in more detail in the more recent map. It contains only a little information on exact topographic heights except for the boundary between land and sea but without information on the vertical datum. Consequently, diverse interpretations are possible. However, the map shows a clear boundary between sea and land. At the beaches in the study area, different shadings are visible. For example, at the beaches *Praia da Ribeira*, *Praia da Rainha* and *Praia da Duquesa*, a darker shaded

**Figure 2.** The historical map of Terzi (1594), highlighting the citadel of Cascais.



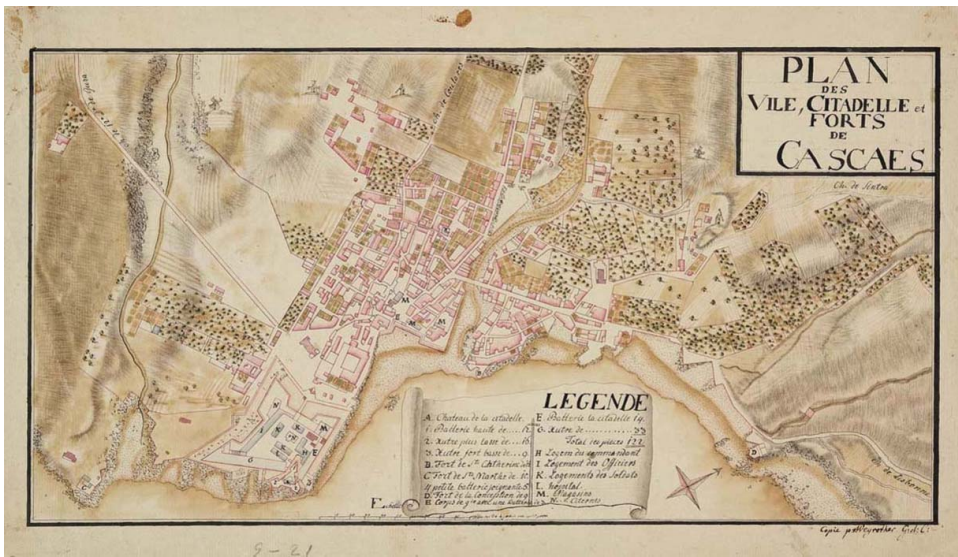


Figure 3. The historical map of Weyröther (n.d.).

strip separates the beaches into two parts. Other topographic features are represented by different shadings but do not deliver explicit elevations.

The hydrographic chart of Da Silva et al. (1879) (Figure 4) is the oldest available hydrographic chart of the area. This map represents the study area before the significant anthropogenic alterations and depicts bathymetric contours with 5 m interval and additional point information. We investigated the sedimentation rates through comparison between present-day and ancient bathymetry in areas not affected by modern construction. The results showed, for this period, differences smaller than 0.2 m confirming that we can neglect sedimentation rates for tsunami simulation purposes. Given this, we considered that this map constitutes the best available representation of the study area at the time of the event.

*Historical accounts.* Marques de Pombal, the prime minister at the time, ordered a national questionnaire to all parishes in the country regarding the earthquake, tsunamis, destruction, and



Figure 4. The part of the city Cascais of the nautical chart, adapted from Da Silva et al. (1879), used for reconstruction.

casualties (see Baptista et al. 1998b for details). Unfortunately, the original accounts of the main areas Lisbon and the South coast disappeared and among them those from Cascais. However, several documents describe the effects in Cascais, namely Pereira de Sousa (1919), and the copy of a document originally written by Brother António do Espírito Santo with the answers to questions formulated by Marques Pombal (Andrade 1956). Other important sources of information are the documents (Henriques 2005, 2014). Boiça et al. (2001) and Carita (2003) describe the fortifications along the coast.

Cascais had a significantly different landscape in 1755 compared to its present shape. The real setup of Cascais in 1755 lies chronologically between these two maps. By analysis and interpretation of the historical maps and accounts, it is possible to describe the former outline of the city. In the historical period, Cascais was a small village, and the centre was near the beach *Praia da Ribeira*. At the beach, *Praia da Ribeira*, the creek *Ribeira das Vinhas* flew into the Atlantic Ocean. Approximately 150 m landward, a bridge connected the western and eastern part of the village (Figures 2 and 3). The other beaches described earlier are also identifiable. The cliffs between the beaches correspond to cliffs also visible in modern satellite imagery. At the citadel, the cliffs show some narrow incisions with sandy inlets according to the old maps.

Key differences between ancient and modern Cascais are the modern Marina and its breakwater, the subterranean channelled creek *Ribeira das Vinhas* and some defense constructions along the coast. The Marina reaches approximately 300 m into the ocean. The main breakwater is about 800 m long, 40 m wide and in some parts higher than 3 m. The breakwater was built in an area where depth was 4–5 m according to ancient hydrographic chart. The subterranean channelled creek *Ribeira das Vinhas* had its river bed at approximately 2–2.5 m above MSL. Nowadays, one of the principle roads in Cascais leads over the channelled stream at 4–7 m above MSL at a length of about 800 m. The significant human interventions altering the landscape in Cascais raise the need of the reconstruction of the PDEM for historical tsunami simulation. We focused our efforts in the reconstruction process in the areas of the Marina, the creek *Ribeira das Vinhas*, and the beaches.

### 3.2. Evaluation and classification of historical topographic change

We focus on a small-scale reconstruction of local and mainly urbanized areas. Growing population and economic activities in the last centuries have led to a considerable modification along the coast. We aim to reconstruct the ancient landscape by combining historical information with present-day data to carry out numerical tsunami modelling on the reconstructed PDEM.

Historical photographs, maps, paintings, and coeval descriptions deliver information and serve at least as a qualitative comparison to more recent maps (Chías & Abad 2009). Studying these historical documents helps to clarify several uncertainties but may also reveal new questions. That may lead to a lengthy investigation process, but it is of utmost importance to get a clear image of a study site in a historical period. Especially, the combination of documents gives a clearer picture of how the study area might have looked like in the desired historical period. Upon the conclusions taken from the historical documents, a comparison with the present-day landscape of the test site reveals the areas where the most significant alterations happened. Field surveys confirmed the conclusions taken from the analysis of the historical documents, making possible the identification of the main differences between the historical period and present-day landscape.

Antique maps are digitized and geo-referenced to present-day satellite images according to the suggestions given in Jenny and Hurni (2011) to estimate the projection of antique maps and transfer their projection. For maps on a local scale, the estimation of the projection is only of minor importance. That is the case for the maps and the clip of the hydrographic chart used regarding the case study in Cascais. To build the PDEM, we need to approximate present-day geomorphologic features to pre-anthropogenic-modified areas like landfills, graded hills, channelled creeks, watercourses, and river mouths. To achieve this, we geo-referenced the maps and the chart to recent satellite images and topographic data. Our historical map is highly accurate showing minimal differences

concerning buildings, rocks, and other features. However, in some areas, for example, at the beaches and the Marina, the shoreline does not coincide with the present-day datasets. Relevant features, such as historical tidal limits or coastlines, can be digitized afterward.

To resolve these discrepancies, we classified the main landforms of the antique map in cliffs, beaches, river-mouths and defined the areas to rebuild the morphology. This process is done manually or automatically using vectorization of raster contents (e.g. scanned historical maps) in a GIS.

The most significant alterations are identifiable comparing the actual landscape of Cascais and new satellite images with the old maps. Nevertheless, on the old map, the topography is often just indicated by shadings without quantitative information. For the main classified features along the coastline and the area of interest, we give examples how to obtain values of topographic heights. These values are used as guidelines to approximate topographic contours along the shadings shown in the antique maps.

### 3.3. PDEM construction

The GIS-based reconstruction process starts with the present-day DEM. We first transformed the datasets to the same reference systems considering vertical datum and map projection. Then, we corrected the depth values to MSL which is 2.08 m above hydrographic zero in Cascais.

In what affects the tsunami impact in coastal areas, we consider and treat separately following classes: coastline (cliffs, beaches, and river mouths/estuaries); creeks and water courses; coastal constructions; and constructions in the inundation area.

#### 3.3.1. Coastline

All historical and recent maps of the coastal area contain quantifiable information. The coastline is the most noticeable feature, and its location defines topographic height zero depending on the vertical datum of the map. Coastlines may have changed within the period because of sea level rise, retreating shorelines or recent constructions. Some historical maps also indicate the intertidal areas using different shadings which are the case for the map used for reconstruction. We interpreted the strip as the intertidal zone. Several reasons confirm this interpretation: cartographers of that time were well aware of the tide phenomena, and today's coastline lies in between low- and high-tide mark but closer to the high-tide mark of the antique map. This interpretation also agrees well with a 0.30 m sea level rise (Antunes & Taborda 2009; Stocker et al. 2013). As a result, we digitized the sea-land boundary as lowest astronomic tide (LAT) mark and the upper limit as high-tide mark of the historical period. The sea level at the time of the 1755 event was about 0.7 m above today's MSL and close to high tide (Baptista et al. 2011). We concluded to use the high-tide mark given in the antique map as the sea-land boundary for the Paleo-DEM; as a consequence, we corrected the recent topographic data to this reference, which is 0.7 m above MSL in Cascais.

*Cliffs.* We suggest to use vertical cross sections in similar geologic ambient for modified or destroyed cliffs along the coastlines. They can be used to obtain mean slopes for the PDEM. Shadings in historical maps also indicate the slope. Depending on the local geology and precipitation regime, local erosion and rates of rock wall retreat should be checked and potentially taken into account. In our case, this is only of minor importance.

Cliffs are reconstructed only in areas where modifications occurred. To rebuild the cliffs where necessary, we suggest using a schematic cross section of the study area representing a typical section of the cliff. If not existent, typical cross sections can be measured using Global Positioning System-Real Time Kinematic (GPS-RTK).

In our study, we manipulated the contour file by deleting the topography of the marina and digitized the low-tide mark given in the antique map (Figure 3). We approximate the topographic height values of the cliffs that need reconstruction according to the typical cross section as presented in Scheffers and Kelletat (2005). These values may vary according to shadings given in the ancient documents and must not necessarily stick to values given in the typical cross section. We drew the



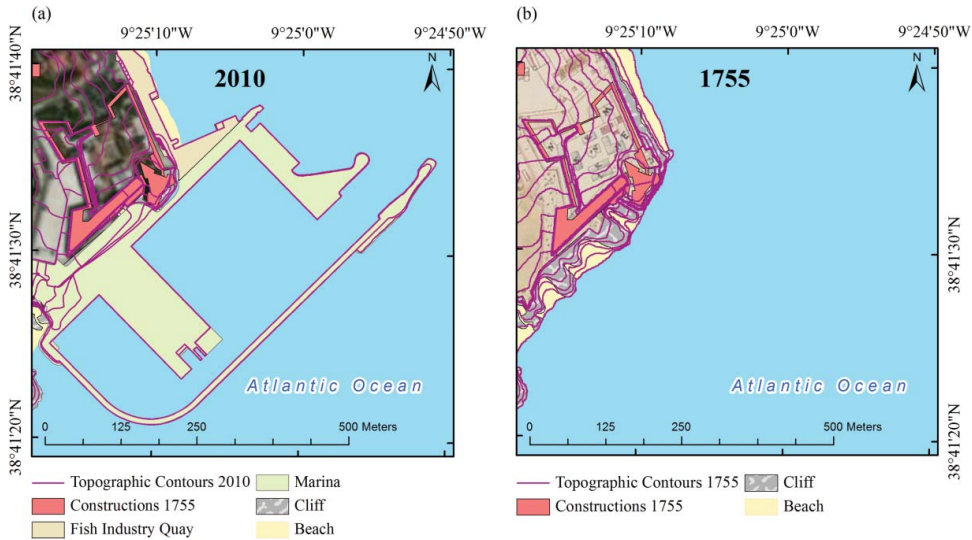


**Figure 5.** (a) Topographic contours of the recent situation including the marina. (b) The identical extent with reconstructed topographic contours along the cliffs before the existence of the marina.

contours according to the shadings of the rocks and the shape given in the historical map and compared the reconstructed parts to old photographs that were taken before the construction of the marina (Henriques 2014). Then, topographic values are attributed to digitized contours. Figure 5 shows an example of the reconstruction of cliffs.

**Beaches.** Morphology and slopes of the beaches may dissipate or amplify tsunami waves. The beach outline, dimensions, and slope must be studied and taken into account in the reconstruction process. The shadings in antique maps along the beaches may indicate the intertidal area along the beaches. By attributing values of high and low water at the margins and by interpolation, one obtains the slope of the beaches. If the antique maps date is not coeval of the event of interest, the variation in the sedimentological budget should be checked and adopted if necessary.

In our study, we focused on the beach *Praia da Ribeira* as coeval sources explain that the tsunami wave entered through the creek's mouth of *Ribeira das Vinhas*. At this beach, the creek *Ribeira das Vinhas* discharged into the Atlantic Ocean where rocky outcrops mark the boundary of the beach. It is a small beach with an extension of about 100 m in length and 50 m width. In the antique map, the beach is larger because of its representation in LAT compared to the satellite image where the sea level is close to MSL. On the old map, we identify that the intertidal margin stretches until the southwestern point of the citadel. We considered a tidal amplitude of about 3.78 m (Da Silva et al. 1879) which results in a slope of approximately 5.4% at the 70-m-wide strip of beach and approximately 18.9% at the 20-m-wide part of the beach. The distance between high- and low-tide mark determines the slope in the intertidal zone. We used these values as reconstruction for the intertidal area of the beach. Figure 6 shows a comparison of a reconstructed beach to its current dimensions.

**River mouths and estuaries.** Regarding big river mouths and estuaries, the reconstruction may depend on the type of estuary in the test site. Reconstructing without hydrographic measurements from the historical period requires intensive studies and detailed chronological analysis of sedimentation, currents and climatological factors of each test site. The method presented relies on implementing historical hydrographic surveys. Point features or bathymetric contours are digitized, and corresponding values are attributed. In some places, more recent hydrographic surveys may complete the old charts. In the case of significant alterations and discrepancies, as in the case of the marina, the present-day dataset is dismissed and replaced by the values of the historical survey.

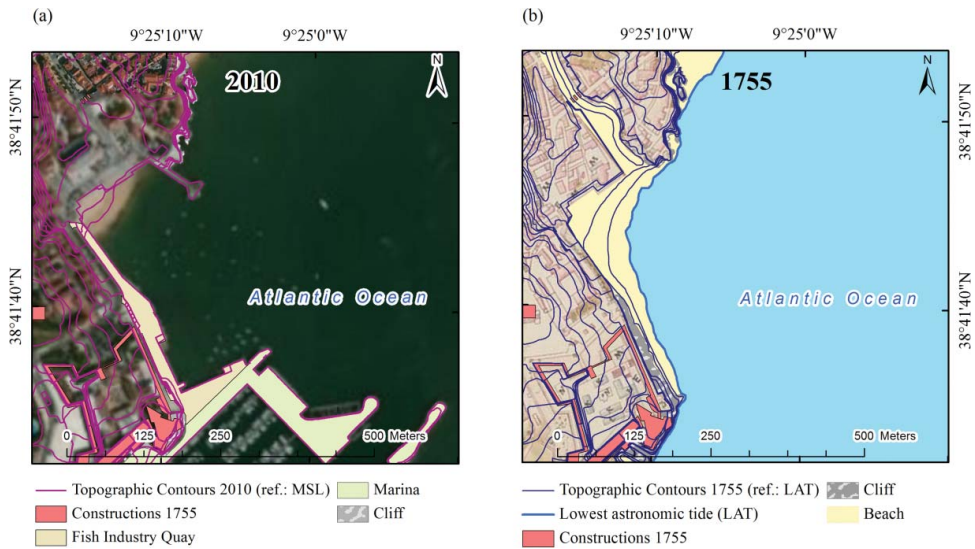


**Figure 6.** (a) Outline and topographic contours of a beach in present-day conditions. (b) Reconstructed topographic contours for 1755.

### 3.3.2. Creeks and water courses

In urban areas, construction works often led to modifications of creeks. A digital renaturation process implements reconstruction of these features. Our approach is to use the digitized boundaries of the creeks in the antique map and the use of GPS-RTK measurements to obtain the slope of the water courses.

In our study area, we rebuilt the old shape and slope of the creek *Ribeira das Vinhas*. We used GPS-RTK on a field survey in Cascais. We measured topographic heights at the creek's mouth and measured 1.7 m above MSL. Approximately 800 m landward, the stream is not subterranean but still channelled. The geo-referenced historical map confirms that the channelled creek is at the same location as the old creek's bed. We measured topographic heights of 2.9 m above MSL at this point assuming that topographic height did not change significantly after the construction works. We interpolated between these two points and implemented the values between the two points in the PDEM.

The creek *Ribeira do Mocho* leads through the agricultural property of the monastery of *Nossa Senhora da Piedade* (Figure 3) surrounded by a fence or a wall at the time of the earthquake. The historical accounts state that the tsunami overtopped the walls and carried two boats inside the property (Andrade 1956). In the Weyröther's map (n.d.), the sandy inlet is displayed as the darker yellowish sand indicating that this area is subject to flooding in high-tide conditions. We assumed that the topography here did not change significantly. To avoid misinterpretation, we did not modify the latest data set at this creek mouth.

Along the creeks, topographic contours are drawn to obtain shape, and slope following the conclusion is taken from the analysis of the GPS measurements. In urban environments, watercourses are often channelled and therefore impossible. In such a case, the contours should be redrawn manually following the course and orthogonal profile as presented in the antique maps.

### 3.3.3. Coastal constructions

Since the middle of 20th century, societies moved closer to the shore. Leisure and economic activities pushed the developments along the sea shore. Harbours, Marinas, sea-defence structures, and hotels transformed natural shorelines, especially in urban areas, into strongly anthropogenic modified landscapes. These structures modified not just topography but also bathymetry and are important

in the reconstruction procedure. Nautical charts from historical bathymetric surveys deliver bathymetric data for reconstruction (Figure 4).

The implemented values from the antique nautical charts replace the deleted contours of these constructions. In case these structures also existed on land, corresponding contours are eliminated and replaced.

To reconstruct the area before the new Marina in our study, we used the hydrographic chart and complemented these with recent bathymetry in deeper areas (Instituto Hidrográfico de Portugal 2012) to obtain higher accuracy.

On the other hand, modern infrastructure also impacted on natural topographic features. These alterations are sometimes interrupting the natural morphology and if so they are clearly noticeable in topographic contours. The combination of the topographic contour file with the shapes of human-made constructions is an even better evidence indicating where construction work has altered the topography. Drawing the contours following their natural course allows reconstructing these alterations. We used these overlaying techniques to correct the landforms according to the shadings presented in the antique maps. The comparison between present-day DEMs and PDEM contours indicates the topographic modifications. Figure 7 depicts an example of a reconstructed area.

For the implementation of the values regarding the different landform classes, we suggest deleting the contours or parts of the point cloud of the present-day DEM within the areas of reconstruction. The antique maps and the interpolation according to the landform class determine the location of the topographic contours.

### 3.3.4. Constructions in the inundation area

An efficient way to collect information on ancient structures is to set up a database that includes all available information. According to the database, buildings can be reconstructed using the available data. After appropriate transformation and referencing processes, it is possible to digitize buildings present in ancient maps. Other documents deliver information on the building heights.

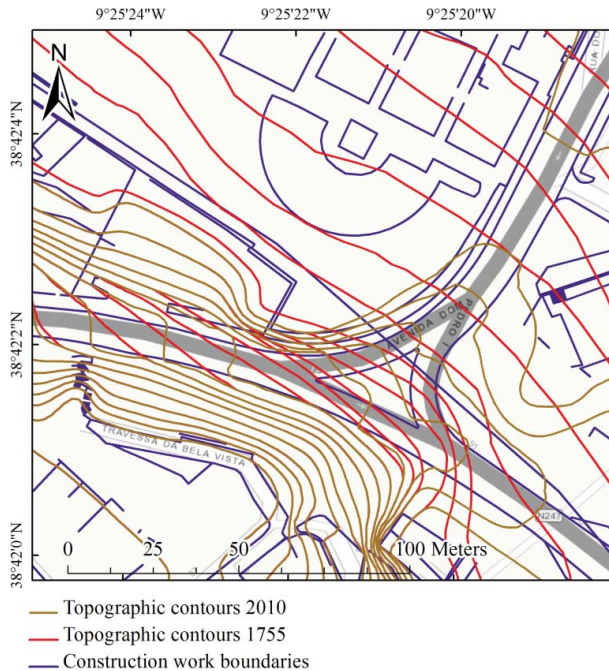


Figure 7. Altered and reconstructed topographic contours due to construction works.

To reconstruct buildings in the area of interest, we suggest to use polylines and polygons and to attribute single height values to each node of structures. A closed polyline limits the buildings' base. The topography around the building gives the topographic values at the building's base. The inner polygon defines the top of the building. The minimum distance of the polygon to the outer polyline is less than 0.1 m. The buildings height plus topographic altitude of the building's base is the topographic height of the inner polygon. Commonly, it is sufficient to simplify structures and to consider a single topographic elevation for the building's top.

During the investigation process, we realized the importance of some existing defense structures from 1640 for tsunami propagation. The antique map depicts the walls built along the fortifications (Figure 8). We investigated which buildings existed in the historical period, and which of these buildings resisted the earthquake. Andrade (1956) and Henriques (2005) present transcripts of coeval documents that served to answer the survey formulated by Marquês de Pombal posterior to the catastrophe. These are detailed descriptions of constructions that withstood the earthquake. Finally, we selected the buildings located in the tsunami impact area and investigated their building heights.

For the reconstructions of buildings, we select only those buildings that did not collapse during the earthquake or where at least reportedly the main walls resisted. Along the fortifications and coastlines, we implemented the defensive walls following the historical map. Figure 8 shows the location of the constructions. The letters in Figures 8 and 12 serve as an identifier of the constructions and correspond to the column ID in Table 2. Table 2 also shows the attributed heights of the

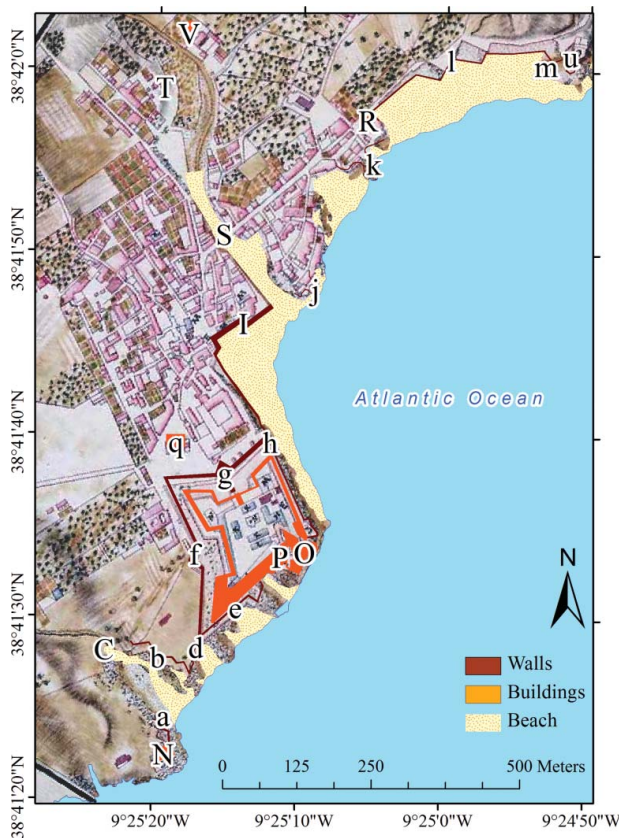


Figure 8. Reconstructed walls and reconstructed buildings digitized upon Weyröther's map (n.d.). The letters upon the walls and buildings correspond to the ID in Table 2.



**Table 2.** Labelled IDs in [Figure 12](#) of the reconstructed walls and buildings and their height used to implement the construction in the PDEM. The capital letters indicate the buildings where inundation was reported.

ID	Wall/buildings name	Height	Source	Reported Inundation
a	Wall of Forte de St. Martha	1.5 m	Boiça et al. (2001)	–
b	Wall of Ribeira do Mocho	2 m	Estimation	–
C	Wall of Piedade Monastery	5 m	Ferreira de Andrade (1956)	Yes
d	Wall of the Citadel	2 m	Estimation	–
e	Wall of the Citadel S	2 m	Estimation	–
f	Wall of the Citadel W	7–9 m	Estimation	–
g	Wall of the Citadel N	7 m	Estimation	–
h	Wall of the Citadel E	7 m	Estimation	–
l	Beach wall	7 m	Boiça et al. (2001)	Yes
j	Wall of Forte St. Catharina	1 m	Estimation	–
k	Wall of Praia de Rainha	1 m	Estimation	–
l	Wall of Praia da Conceição	1 m	Estimation	–
m	Wall of Forte de Conceição	1 m	Estimation	–
N	Forte da St. Martha	3.5 m	Estimation	Yes
O	Fortress	4–8 m	Still existent	Not inside
P	Citadel	5–19 m	Still existent	Not inside
q	Igreja da Assumpção	6 m	Still existent	No
R	Capela da Conceição	2–3 m	Still existent	Yes
S	Pillars of the bridge	6 m outer pillars, 8 m central pillar	Ferreira de Andrade (1956)	Yes
T	Poço velho (The old well)	–	–	Yes
u	Forte da Conceição	3.5 m	Estimation	–
V	Quinta St. Clara	–	–	Yes

buildings and walls. The map in [Figure 8](#) also indicates the location of the old well (*Poço Velho*) and the farm *Quinta da Santa Clara* – both areas which were reached by the tsunami according to reports. We could not find additional information on these buildings and did not include them in the PDEM.

We implemented the buildings using two nearly overlaying polygons to obtain vertical walls of the constructions in the PDEM, as suggested earlier. Therefore, building heights were treated as topography within the PDEM. For 3D visualization of structures, we used extrusion of the base polygons in GIS before computing the final PDEM.

After implementing necessary alterations in the GIS, the dataset contains several points, polyline and polygon files. Each of these files is composed of several features providing topographic height information. This composition of data is rendered to a Triangulated Irregular Network (TIN) and displayed in 3D for verification. When necessary, contours, points or polygons can be adopted or modified to produce a new TIN. We repeat the verification process until the TIN is representing the study area in the desired shape. The final TIN is used to compute the PDEM in a grid format in the defined resolution for numerical tsunami modelling. [Figure 9](#) shows the contours of the current DEM and all alterations to reconstruct the PDEM. [Figure 11](#) depicts the final PDEM grid with 2-m resolution.

#### 4. Tsunami simulation

We used the code COMCOT (Cornell Multi-grid Coupled Tsunami Model; Liu et al. 1998; Wang 2009). To obtain a 2-m resolution grid at the study area, we used a system of four nested grids. The advantage of using nested grid is the saving of computation time. We used a refinement factor of four to do the nesting from 128-m cell size towards the final grid size of 2 m.

In the tsunami source area, corresponding to the Southwest Iberian Margin (SWIM) ([Figure 10](#)), we used GEBCO (2014) bathymetry to generate a 128-m cell size grid. The intermediate grids have a resolution of 8 and 32 m, respectively ([Figure 10](#)).

COMCOT code allows passing the wave motion through the boundaries from one domain to another with minuscule reflections (Wang 2009). The code solves linear and non-linear approximations of shallow-water equations (SWEs) to calculate tsunami propagation and inundation in a



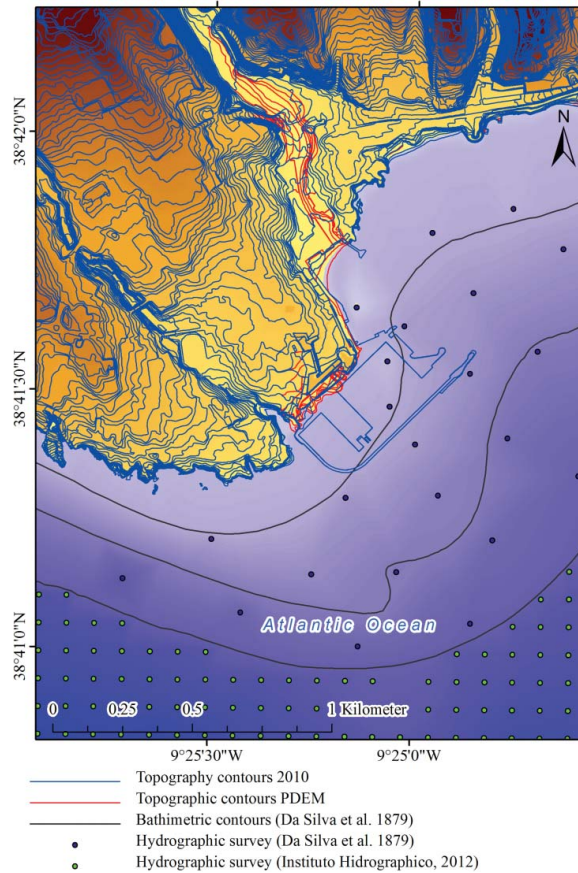


**Figure 9.** Topographic contours of 2010 were modified to obtain the topographic contours of the PDEM. The bathymetric contours and points of the hydrographic survey have been digitized from the nautical chart (Da Silva et al. 1879). The southern part of the bathymetry is complemented by the bathymetric model of Cascais (Instituto Hidrográfico de Portugal 2012).

Cartesian or spherical reference system. The moving boundary algorithm based on wet and dry cells implemented in the code (Liu et al. 1995) computes the inundation in the PDEM.

To launch the tsunami simulation, we use two initial conditions: the initial sea surface elevation and the velocity at instant  $t = 0$  s. We used Mansinha and Smylie (1971) half-space elastic theory embedded in Mirone suite (Luis 2007), to calculate the sea bottom deformation, caused by the earthquake. To compute the initial sea surface elevation we assume that it is equal to the ocean bottom deformation (assuming the water as incompressible fluid). At time  $t = 0$  s, the velocity field is zero. To simulate a 1755-like event, we need to compute the earthquake scenario that causes the tsunami. To do this, we used the source and fault parameters presented by Baptista et al. (2011) (Table 3). That corresponds to an 8.4-magnitude earthquake at the Horseshoe Fault (HSF) (Figure 10).

We set the model to the reference of the tide conditions in 1755 at tsunami arrival (Baptista et al. 2011) which is 0.7 m above today's MSL. We ran the simulation model for four hours of tsunami propagation to compute a map depicting the maximum wave amplitude (MWA) and maximum flow depth (MFD) in the study area. We set the Manning roughness coefficient to zero in the first three layers. In the final layer, the PDEM where friction and non-linear effects are getting more important, we used a Manning roughness coefficient of  $n = 0.025$ . Additionally, we used three virtual tide gauges to record the synthetic waveforms of the produced tsunami. Figure 10 depicts the locations of the tide gauges.

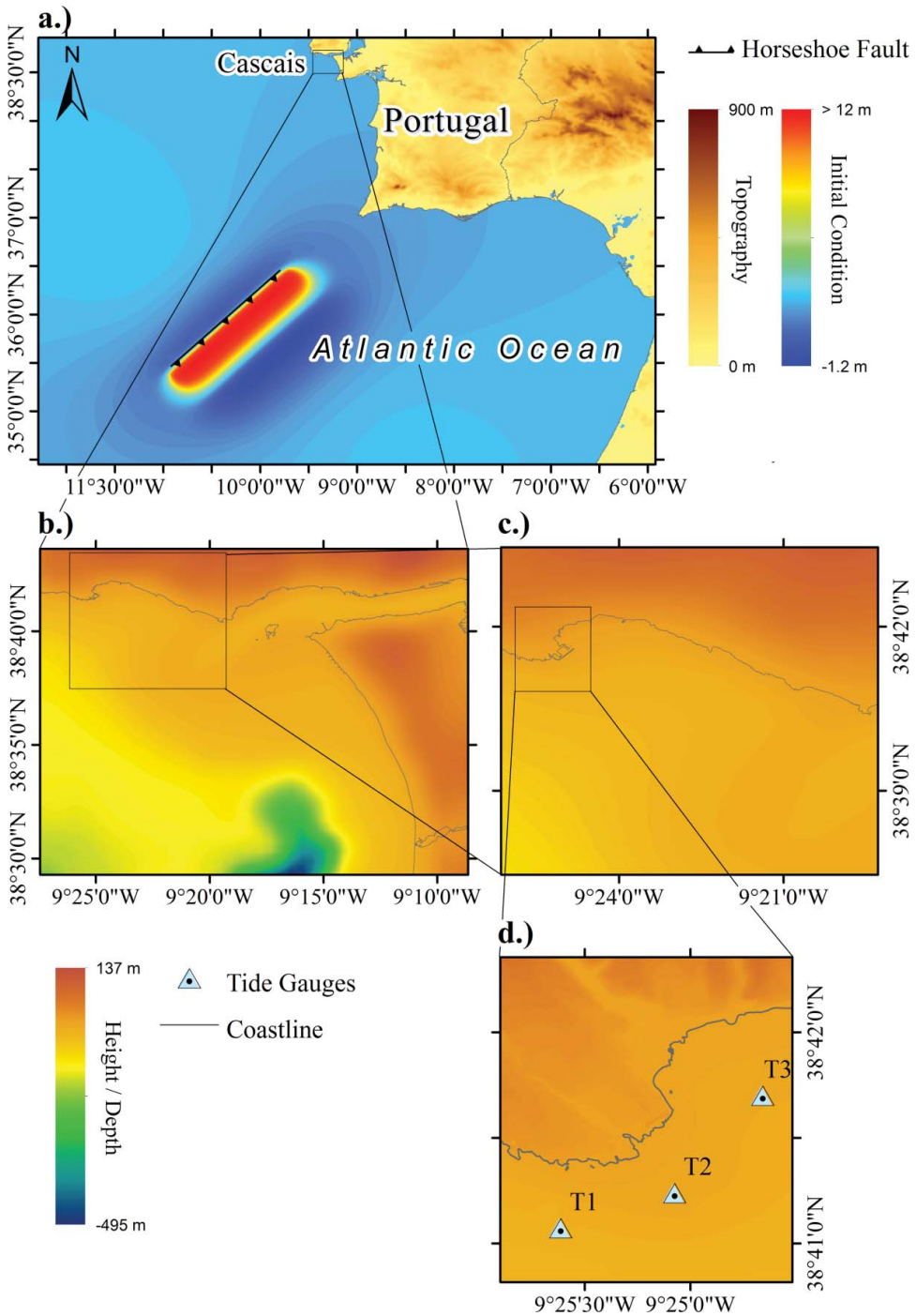


**Figure 10.** Four nested grids used for numerical tsunami modelling. (a) The Southwest Iberian Margin (SWIM) and the 1755 candidate source Horseshoe Fault and the corresponding initial condition for tsunami propagation; (b) and (c) the intermediate grids used in the numerical tsunami simulation with 32-m and 8-m resolution, respectively; (d) the final grid of 2-m resolution computed using the PDEM; the points T1, T2 and T3 show the locations of the virtual tide gauges.

**Table 3.** Fault parameters for a 1755-like scenario.

Fault	L (km)	W (km)	Rake (°)	Strike (°)	Dip (°)	Slip (m)	Depth (km)	$\mu$ (Pa)	Mw
HSF	165	70	90	42.1	35	15	5	3e+10	8.4

## 5. Results

Here we present the results divided into the results of the PDEM reconstruction and the results of numerical tsunami modelling.

### 5.1. Results of the PDEM reconstruction

The reconstructed PDEM covers an area of 5.7 km<sup>2</sup>. Above 20 m, no features had been altered. The reconstructed area reaches approximately 0.8 km inland at the creek *Ribeira das Vinhas* (Figure 9). In this area, the channelled creek had been re-naturalized according to the values measured in the field survey. We digitized the boundaries of the creek according to the antique map. We deleted the Marina and reconstructed antique bathymetry according to the data of the historical nautical chart and the cliffs at the area of the Marina following a predominant slope between 10% and 15%. We imported the information on the beaches and obtained a beach slope values between 1% and 15% at the boundaries. We reconstructed the channelled creek *Ribeira das Vinhas* to the shape of the historical period which corresponds to a slope of  $\sim 0.15\%$  along the borders of the ancient map. Apart from deleting the recent constructions, we reconstructed the buildings and walls given in Table 2 according to values found in historical sources or based on estimations. The biggest wall at the beach *Praia de Ribeira* has a height of 7 m and reaches a topographic height of 10 m.

We also implemented defense structures like the citadel and smaller walls along the shoreline. The PDEM represents most of the features but the walls of smaller dimension from the fort along the monastery *Nossa Senhora da Piedade* and the walls of fort *Forte de St. Catharina* to the fort *Forte*

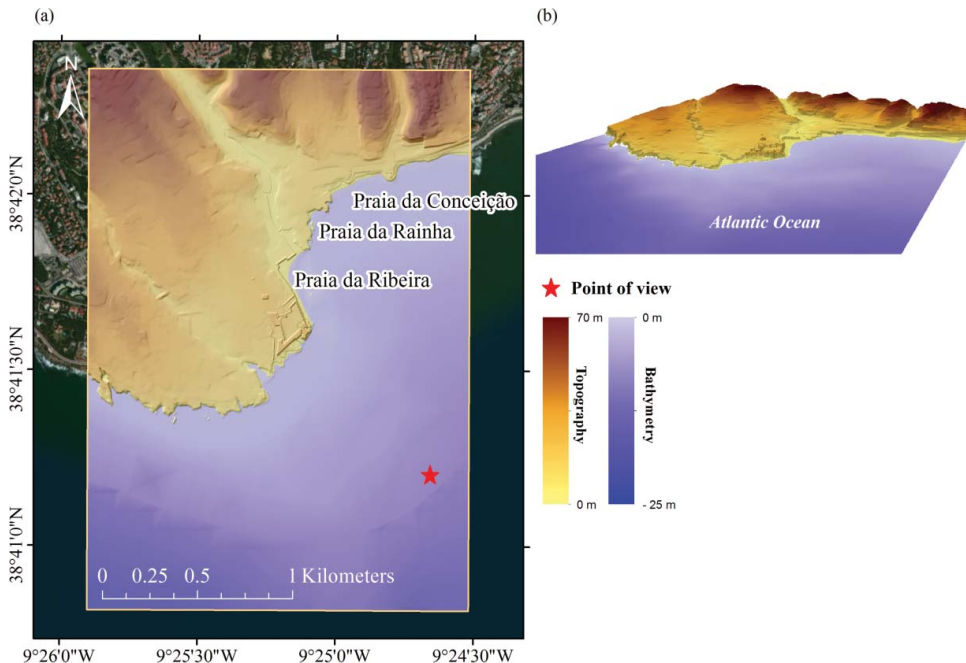


**Figure 11.** (a) Hill-shade of the reconstructed PDEM of the Cascais study area. (b) 3D view from the southeast marked by the red star in (a).

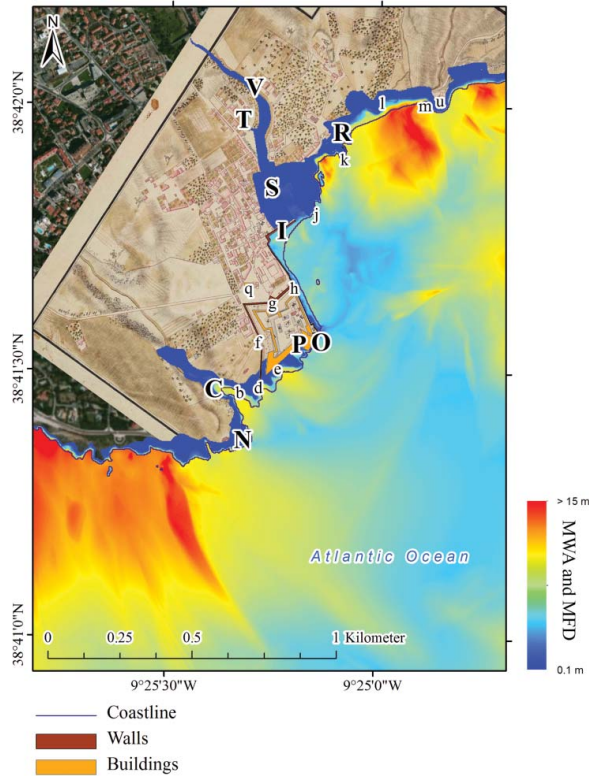


**Figure 12.** Maximum wave amplitude (MWA) and maximum flow depth (MFD) above the geo-referenced map (Weyröther n.d.) and the reconstructed walls and buildings in the study area of Cascais. The capital letters indicate the reportedly inundated buildings.

*de Conceição* suffer from the 2-m final grid resolution. The tsunami simulation requires a regular space grid, and hence the PDEM had been transferred to a grid format. **Figure 11** shows the results of the PDEM reconstruction.

## 5.2. Results of the tsunami simulation

We ran the numerical model using the reconstructed PDEM of Cascais for 1755. Using the results of the tsunami simulation, we built a map depicting MWA and MFD (**Figure 12**). The letters in **Figure 12** correspond to the identifiers of the constructions of column ID in **Table 2**. The capital letters in **Figure 12** identify the reportedly inundated structures. **Table 2** also indicates flooded buildings. **Figure 13** presents the results of the synthetic waveforms recorded at the virtual tide gauges T1, T2, and T3. The flow depth is the water column on dry land, and the wave amplitude is the water column above sea level defined in the PDEM for the 1755 tsunami.

In the study area, we have a total inundation area of about 0.20 km<sup>2</sup>. The waves penetrated about 0.8 km inland at the creek *Ribeira das Vinhas* passing and partially inundating the area of the farm *Quinta da Santa Clara* (ID V in **Table 2** and **Figure 12**). This farm was located approximately 0.5 km inland. The tsunami simulation also shows overtopping of the two outer pillars of the bridge. MFD values are about 3.9 m around the pillars of the bridge. According to the tsunami simulation, the waves did reach near the location of today's entrance old well (*Poço Velho*) (ID T in **Table 2** and **Figure 12**). The entrance lies at a topographic height of about 7 m. The distance between the limit of the inundation area to the old well is 40 m (ID T in **Table 2** and **Figure 12**). Highest MFD values occur at the beaches with values above 7 m at the beach *Praia da Ribeira* and above 9 m at the other

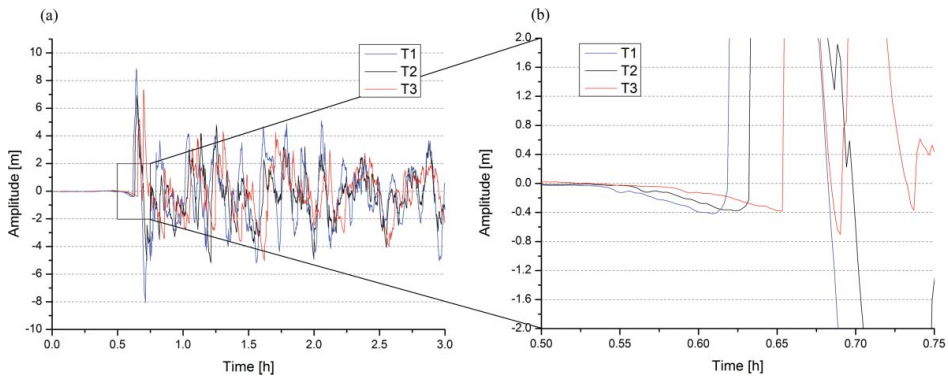


**Figure 13.** (a) Synthetic waveforms recorded at the virtual tide gauges T1, T2, T3 computed for a tsunami simulation with 3 h propagation time. (b) Zoom-in to the timespan 0.5–0.75 h showing the 0.4 m drawdown before the tsunami arrival.

beaches. The analysis of the results also indicates that the waves overtopped all the walls of smaller dimensions. But the tsunami did not exceed parts of the largest beach wall (ID I in Table 2 and Figure 12). Behind this barrier, MFD values reach up to 0.2 m. The waves did not enter the citadel or the fort, but MFD values reach 2.5 m along the south-eastern part of the citadel. Also, at the creek *Ribeira do Mocho*, the tsunami penetrated approximately 0.35 km inland and entered the area of the monastery *Nossa Senhora da Piedade*. The tsunami simulation computed MFD values of above 6 m at the wall of the monastery at the creek *Ribeira do Mocho* (ID C in Table 2 and Figure 12). The tsunami simulation inundated the areas of the fort *Forte de Santa Martha*, the fort *Forte de Conceição*, and the chapel *Capela de Conceição*. The MFD values at the chapel vary between 0.1 and 1.8 m. However, the MFD at the side of the entrance of the chapel is about 1 m. Figure 12 presents the results of the tsunami simulation.

The virtual tide gauges recorded at the points T1–T3 show MWA of about 10 m in front of the beach *Praia da Ribeira*. Figure 13 shows the synthetic waveforms. The tsunami approached the coast from the southwest with the first signal at tide gauge T1 after about 30-min tsunami travel time (Figures 10 and 13). The first movement of the incident wave at the three tide gauges is downward of about 0.4 m in approximately 10 min (Figure 13(b)). The following movement is a fast upward movement, and the biggest wave recorded at the virtual tide gauges T1 and T2 with 9 and 7 m, respectively. The recorded period is about 8 min. After 3 h, the amplitude is still about 4 m.

## 6. Discussion

We present a methodology to reconstruct recent Holocene PDEM in an urban environment and apply it to the coastal city of Cascais for the historical period 1755. We finally used the reconstructed PDEM for the tsunami simulation caused by a 1755-like event. However, PDEM reconstruction is not limited to numerical tsunami modelling. Reconstructed PDEMs can also be useful in other studies or applications.

### 6.1. Discussion of the PDEM

We investigated on the outline of the city in the historical period and combined historical information with modern GIS technologies. We compared the city today with its shape in the historical period and identified the differences. Upon these differences, we classified the different landforms and reconstructed the topography and bathymetry following the consideration of each class. Additionally, we included walls and buildings present in the study area at the time in the PDEM (Figure 8).



The key areas of reconstructions were the beaches, the cliffs along the citadel, the Marina, and the creek *Ribeira das Vinhas* (Figure 9). The final result consists in a PDEM with a final resolution of 2 m representing topography, bathymetry and implemented buildings (Figure 11).

We focused our study on how far is it possible to reconstruct topography, bathymetry, and buildings of a seriously anthropogenic modified landscape. The existence of historical maps, charts, and other documents facilitates this process but also may lead to several ambiguities.

- Maps and charts can be geo-referenced, but their accuracy is difficult to evaluate. We digitized the sea–land boundary shown in Weyröther (n.d.) as LAT although this reference is not given in the antique map. However, several indicators favour our interpretation. In this map, an intertidal area is clearly indicated by different shadings of the beaches. The distance of the sea–land boundary to the shaded area is in the same order of magnitude as today’s horizontal distance of LAT to HCW (highest charted water). The maximum amplitude of the tides is constant which underlined our interpretation that shaded area in the map is depicting the intertidal area. The comparison to the antique nautical chart also shows an equally large beach at the beach *Praia da Ribeira*. This chart includes information on the maximum and minimum tidal amplitude, referenced to the lowest tidal amplitude in a maximum tide. This information was essential to establish the reported high-tide condition of the event.
- Which of the buildings shown in the maps resisted the earthquake? To solve this, we relied on further source of information. In our study area, coeval documents state enormous destruction. Andrade (1956) and Henriques (2005) present transcripts of these sources including information on walls and buildings that resisted. We implemented these walls and buildings in the PDEM according to the historical map (Figures 8 and 12 and Table 2). In case building heights were not available, we estimated them.
- Certain assumptions are necessary to reconstruct morphology. For the cliffs, we compared slope values of a typical cross section to draw the topographic contours in areas where reconstruction was needed. For creeks, we suggested applying a comparative method using GPS-RTK at creeks in similar ambient to estimate mean slope values of their final course before flowing into the sea. However, for the presented case study, creeks in the same ambient were non-existent and we interpolated values between two measured references. We digitized the creek boundaries from geo-referenced historical maps and implemented the slope values redrawing the topographic contours. A qualitative verification of morphology in some parts of the PDEM was possible by comparison with old photographs presented in Henriques (2014).

The investigation in historical documents and field surveys play an essential element of the research process. Without the detailed analysis and the combination of various sources and information, it would not have been possible to approximate the landscape of a study area in the historical period 1755. Numerous assumptions were necessary to reconstruct the PDEM, and it is hard to quantify its accuracy.

We transferred the resulting PDEM to grid format with 2-m resolution (Figure 11). This final resolution is necessary to represent the walls and buildings in the PDEM. Therefore, morphologic features are described in very high detail, but some of the walls with smaller dimensions suffer from the chosen resolution. However, a higher resolute PDEM results in a longer computation time for the tsunami simulation.

## 6.2. Discussion of the tsunami simulation

To simulate a 1755-like event, we used the PDEM and a non-linear shallow water code to propagate the tsunami from the source area towards the coast and the rupture of the HSF as earthquake scenario (Omira et al. 2009, 2010; Baptista et al. 2011).

A study commissioned by the Municipality of Cascais to assess tsunami hazard in the area shows inundation depths greater than 1 and 12 m for earthquake scenarios of magnitudes 8.0 and 8.8 in the Horseshoe fault (Câmara Municipal de Cascais – Serviço Municipal de Protecção Civil 2015). However, these results cannot be compared directly because of the extensive modifications of the site.

Our results show a massive impact in the study area with inundation depths greater than 9 m in the study area. These results are compatible with all of the descriptions by coeval sources regarding the tsunami:

- Coeval sources state the tsunami reached the farm *Quinta de Santa Clara* (ID V in Table 2 and Figure 12). The tsunami simulation computed inundation penetration in some parts of the farm and 0.25 km further inland, which is in agreement with the historical reports.
- According to coeval sources, the tsunami reached the old well *Poço Velho* (ID T in Table 2 and Figure 12). And other documents describe that the water of the old well was not useable due to salinization after the tsunami. The tsunami simulation shows that limits of inundation reach close (40 m) to the old well. It is a small system of a grotto of approximately 50 m length, and the tsunami might have penetrated the subterranean caves.
- According to the coeval description, the tsunami overtopped the walls of the monastery *Nossa Senhora da Piedade* placing two boats inside the walls. Tsunami modelling shows that the waves penetrated further inland than the location of the wall (ID C in Table 2 and Figure 12). MFD values at the site of the wall are of about 5–6 m and the wall had a height of approximately 2 m according to descriptions. Therefore, the waves could have indeed placed the boats inside the monastery. However, one should note that the wall's width is less than 1 m and therefore it is not precisely represented by the PDEM.
- At the chapel *Capela de Conceição*, the waves reached the entrance but could not enter and the people who took shelter inside reportedly survived (Pereira de Sousa 1919; Andrade 1956). Indeed, people could have survived inside. The tsunami simulation computed MFD values of about 1 m at the entrance of the chapel. At the western side of the chapel, MFD values are about 0.5 m, and there is a small area of about 100 m<sup>2</sup> without inundation. In the PDEM, the entrance is situated at a topographic height of about 7 m and the chapel is located close to the Beach *Praia de Conceição* (ID R in Table 2 and Figure 12). Nevertheless, the MFD value of 1 m might be slightly too high at the entrance of the chapel *Capela de Conceição*. Underestimation of the height of the walls along the beach *Praia de Conceição* (ID I in Table 2 and Figure 12) is a possible explanation for the discrepancies of the coeval sources and the tsunami simulation. Also, the width of this wall is less than 2 m and therefore not sufficiently represented in the PDEM.
- Reports state that the first movement of the tsunami was downwards (Andrade 1956; Henriques 2005). The synthetic waveforms at the virtual tide gauges confirm this observation (Figure 13(b)). The small drawdown of 0.4 m may not seem to be significant in comparison to the 9-m wave height. A drawdown of 0.4 m within 10 min at a beach 0.1 degree slope is equal to a drawback of about 4 m. That is in good agreement with the coeval sources that state a drawback of several metres before the wave struck.
- The tsunami simulation also confirms the reported tsunami travel time of about half an hour (Baptista et al. 1998a). The downward movement started slowly at about 30 min. After 35 min, the waves with MWA of 7–9 m measured at the virtual tide gauges hit the shore (Figure 13).
- The tsunami simulation did not show overtopping of the largest beach wall (ID I in Table 2 and Figure 12) at the beach *Praia da Ribeira*. Behind this wall, the MFD are up to 0.2 m. The PDEM clearly represents this wall with 7 m height and 6–8 m width.
- Coeval sources indicate the tsunami did not enter the citadel and the fort. Our tsunami simulation confirms these reports. Along the citadel and the fort (ID P and O in Table 2 and

Figure 12), the tsunami could not penetrate further inland. These massive structures might have acted as obstacles to the impacting waves and possibly prevented an even worse catastrophe in 1755.

## 7. Conclusions

We present a methodology for PDEM reconstruction in an urban environment on the base of a case study. This method consists in redefining topography and bathymetry of the present-day DEM by the implementation of historical data. Historical data are rare and mainly existing in urban environments for historically important locations. For these areas, a PDEM may help for a better understanding of historic events. Through evaluation and classification of different landforms in the datasets, areas of reconstruction are identified. We implemented existent topographic and bathymetric values in the PDEM. If no absolute values were available, we used interpolation between known values and redrew the contours according to the antique map.

The use of the methodology of PDEM reconstruction enables us to model, for example, historic tsunami events in an urban environment. By applying PDEM reconstruction and numerical tsunami modelling, we could reproduce all occurrences due to the tsunami as described by coeval sources in Cascais in 1755. In the area of the chapel, our results diverge slightly from the description in the historical accounts.

As the 1755 earthquake and tsunami is a historic event, the location of the source is estimated (c.f. Baptista & Miranda 2009b). Applying PDEM reconstruction on various test sites where reports of the 1755 tsunami exist, and numerical tsunami simulation, may help for a better discrimination of the tsunami source.

Finally, the methodology of reconstruction of PDEMs presented is also valid in different geomorphological environments. The PDEM is a necessary tool to simulate physical phenomena in historical periods, and its quality is of importance to reproduce similar historic events. The PDEM will help to reveal new information on historic events where only little data is available.

## Acknowledgments

The authors wish to thank Cascais Municipality for providing the digital topographic data and Dr Carlos Antunes for his help in interpreting the historical maps. Finally, the authors thank the reviewers for their comments and suggestions, which greatly improved the study.


## Disclosure statement


No potential conflict of interest was reported by the authors.


## Funding

This work is funded by ASTARTE – Assessment, Strategy and Risk Reduction for Tsunamis in Europe – FP7-ENV2013 6.4-3 [grant number 603839].

## ORCID

Martin Wronna  <http://orcid.org/0000-0002-8773-3738>

Maria Ana Baptista  <http://orcid.org/0000-0002-6381-703X>

Joachim Götz  <http://orcid.org/0000-0002-3423-445X>

## References

- Andrade F. 1956. A vila de Cascais e o terremoto de 1755. [The city of Cascais and the earthquake of 1755]. *Cascais e seus lugares: revista cultural da Junta de Turismo de Cascais*. p. 29–63.
- Antunes C, Taborada R. 2009. Sea level at Cascais tide gauge: data, analysis and results. *SI 56 Proceeding of the 10th International Coastal Symposium*. Lisbon: ISBN; p. 218–222.
- Baptista MA, Heitor S, Miranda JM, Miranda P, Mendes Victor L. 1998a. The 1755 Lisbon tsunami: evaluation of the tsunami parameters. *J Geodyn*. 25:143–157.
- Baptista MA, Miranda JM. 2009a. Revision of the Portuguese catalog of tsunamis. *Nat Hazards Earth Syst Sci*. 9:25–42.
- Baptista MA, Miranda JM. 2009b. Evaluation of the 1755 earthquake source using tsunami modeling. *The 1755 Lisbon Earthquake: revisited*. Springer; p. 425–432. Available from: [http://dx.doi.org/10.1007/978-1-4020-8609-0\\_27](http://dx.doi.org/10.1007/978-1-4020-8609-0_27)
- Baptista MA, Miranda PMA, Miranda JM, Victor LM. 1998b. Constrains on the source of the 1755 Lisbon tsunami inferred from numerical modelling of historical data on the source of the 1755 Lisbon tsunami. *J Geodyn*. 25:159–174.
- Baptista MA, Miranda JM, Omira R, Antunes C. 2011. Potential inundation of Lisbon downtown by a 1755-like tsunami. *Nat Hazards Earth Syst Sci*. 11:3319–3326.
- Blakemore M, Harley J. 1980. Concepts in the history of cartography. A review and perspective. Vol. 17/4, Monograph 26 von. *Cartographica*, International Publications on Cartography.
- Boiça JMF, Barros MFR, Ramalho MM. 2001. *As fortificações marítimas da Costa de Cascais* [The forts along the coast of Cascais]. Lisboa: Quetzal. ISBN 972-564-509-X.
- Boutoura C, Livieratos E. 2006. Some fundamentals for the study of the geometry of early maps by comparative methods. *e-Perimtron*. 1:60–70.
- Carita R. 2003. *Citadela de Cascais (Pedras, Homens e Armas)* [The citadel of Cascais (stones, men and weapon)]. Lisbon: Estado-Maior do Exército Direcção de Documentação e História Militar.
- Câmara Municipal de Cascais – Serviço Municipal de Protecção Civil. 2015. *Dossiê de Susceptibilidade* [Dossier of susceptibility] [Internet; cited Sep 2016]. Available from: [http://www.cm-cascais.pt/sites/default/files/anexos/gerais/new/02\\_relatorio\\_0.pdf](http://www.cm-cascais.pt/sites/default/files/anexos/gerais/new/02_relatorio_0.pdf)
- Chías P, Abad T. 2009. GIS tools for comparing historical and contemporary landscapes through local map series. *e-Perimtron*. 4:61–72.
- Da Silva FMP, Batalha CM, De Vasconcelos CFB, Lewicki J, Folque F. 1879. *Plano Hydrographico da Barra do Porto de Lisboa* [Hydrographic chart of the bar and port of Lisbon]. Collected Data from 1842, 1843 and 1845 ordered by her majesty [map]. Scale 1:20000. Lisbon: Deposito Hydrographico. Biblioteca Nacional de Portugal, pressmark C.C. 996 R. [Internet]. [cited 2016 Apr 4.] Available from: <http://purl.pt/16765>
- [GEBCO] The General Bathymetric Chart of the Oceans. 2014. *GEBCO\_2014 grid*, version 20150318. [Internet; cited Mar 2016]. Available from: <http://www.gebco.net>
- Heidarzadeh M, Pirooz MD, Zaker NH, Yalciner AC. 2009. Preliminary estimation of the tsunami hazards associated with the Makran subduction zone at the northwestern Indian Ocean. *Nat Hazards*. 48:229–243.
- Henriques JM. 2005. *Cascais em 1755: do terramoto à reconstrução* [Cascais in 1755: from the earthquake to reconstruction]. Cascais: Câmara municipal de Cascais. ISBN 972-637-154-6.
- Henriques JM. 2014. *Cascais. 650 anos de história* [Cascais. 650 years of history]. Cascais: Câmara municipal de Cascais.
- Instituto Hidrográfico de Portugal. 2012. *Modelo Batimetrico de Cascais* [Bathymetric model of Cascais]. [Internet; cited 4 Apr 2016]. Available from: <http://www.hidrografico.pt/download-gratuito.php>
- James LA, Hodgson ME, Ghoshal S, Latiolais MM. 2012. Geomorphic change detection using historic maps and DEM differencing: the temporal dimension of geospatial analysis. *Geomorphology*. 137:181–198.
- Jenny B, Hurni L. 2011. Studying cartographic heritage: analysis and visualization of geometric distortions. *Comput Graph*. 35:402–411.
- Jenny B, Weber A, Hurni L. 2007. Visualizing the planimetric accuracy of historical maps with MapAnalyst. *Cartographica: Int J Geogr Inf Geovisual*. 42:89–94.
- Kormann M, Lock G. 2013. *Dynamic models to reconstruct ancient landscapes* [Internet]. [cited 2016 Apr 4]. Available from: <http://shura.shu.ac.uk/5285/>.
- Liu PLF, Cho YS, Briggs MJ, Kanoglu U, Synolakis CE. 1995. Runup of solitary waves on a circular island. *J Fluid Mech*. 302:259–285.
- Liu PLF, Woo SB, Cho YS. 1998. *Computer programs for tsunami propagation and inundation*. Cornell University. [Internet; cited 25 May 2016]. Available from: [http://tsunamiportal.nacse.org/documetation/COMCOT\\_tech.pdf](http://tsunamiportal.nacse.org/documetation/COMCOT_tech.pdf)
- Luis JF. 2007. Mirone: a multi-purpose tool for exploring grid data. *Comput Geosci*. 33:31–41.
- Mansinha L, Smylie DE. 1971. The displacement fields of inclined faults. *Bull Seismol Soc Am*. 61:1433–1440.
- Martins I, Victor LM. 1990. [Contribution to the studies of seismicity of Continental Portugal]. Lisboa: Instituto Geofísico do Infante D. Luís, Universidade de Lisboa.
- Omira R, Baptista MA, Matias L, Miranda JM, Catita C, Carrilho F, Toto E. 2009. Design of a sea-level tsunami detection network for the Gulf of Cadiz. *Nat Hazards Earth Syst Sci*. 9:1327–1338.

- Omira R, Baptista MA, Miranda JM, Toto E, Catita C, Catalao J. 2010. Tsunami vulnerability assessment of Casablanca–Morocco using numerical modelling and GIS tools. *Nat Hazards*. 54:75–95.
- Omira R, Zourarah B, Leone F, Cherel JP, Baptista MA, de Richemond NM, Mellas S. 2012. Can numerical modeling clarify the uncertainties of historical reports? *Tsunami - analysis of a hazard - from physical interpretation to human impact*. doi: 10.5772/51864.
- Pereira de Sousa FL. 1919. O terremoto do 1º de novembro de 1755 em Portugal, um estudo demografico [The 1st November 1755 Earthquake in Portugal, a demographic study]. Vol. I and II. *Serviços Geológicos de Portugal*.
- Scheffers A, Kelletat D. 2005. Tsunami relics on the coastal landscape west of Lisbon, Portugal. *Sci Tsunami Hazards*. 23:3–16.
- Stocker TF, Qin D, Plattner GK, Tignor MMB, Allen SK, Boschung J, Nauels A, Xia Y, Bex V, Midgley PM. 2013. *Climate change 2013: the physical science basis. Contribution of Working Group I to the Fifth Assessment Report of the Intergovernmental Panel on Climate Change (AR5)*. New York (NY): Cambridge University Press.
- Terzi F. 1594. Plano de Cascaes en donde figuran en perspectiva las fortalezas nueva y vieja así como las Casas de D. Antonio, señor de Cascaes [map]. Scale in 100 Braças equivalent to 220 m. *Archivo General de Simancas*. Ministerio de Cultura, Archivos Estatales. Pressmark. MPD, 12, 161.
- Wang X. 2009. User manual for COMCOT version 1.7 (first draft). [Internet]. New Zealand: Institute of Geological & Nuclear Science; [cited 2016 May 25]. Available from: <https://pdfs.semanticscholar.org/401d/e93588d6c28d0c3984044ad1f95b75dadab0.pdf>
- Weyröther GC. n.d.. Plan des villes, Citadelle et Forts de Cascaes [map]. Scale not given. Ca. 1800. *Direção dos Serviços de Engenharia – Gabinete de Estudos Arqueológicos de Engenharia Militar*. Arquivo Histórico Militar.
- Wijetunge JJ. 2014. A deterministic analysis of tsunami hazard and risk for the southwest coast of Sri Lanka. *Cont Shelf Res*. 79:23–35.
- Wronna M, Omira R, Baptista MA. 2015. Deterministic approach for multiple-source tsunami hazard assessment for Sines, Portugal. *Nat Hazards Earth Syst Sci*. 15:2557–2568.